JAAS

PAPER

View Article Online
View Journal

Cite this: DOI: 10.1039/c7ja00405b

Investigation of spectral interference in the determination of Pb in road dust using high-resolution continuum source graphite furnace atomic absorption spectrometry and direct solid sample analysis†

Susane Schossler Fick,[a] Flávio Venâncio Nakadi,[a] Fabian Fujiwara,[b] Patricia Smichowski,[b] Maria Goreti R. Vale,*[ac] Bernhard Welz[cd] and Jailson B. de Andrade[c]

Direct solid sample analysis using graphite furnace atomic absorption spectrometry (GF AAS) is an attractive alternative because no sample pretreatment is necessary. However, the major obstacles of this technique are spectral interference and the limited background correction capability of conventional line source AAS instruments. The introduction of high-resolution continuum source atomic absorption spectrometry (HR-CS AAS) has brought about a significant change in this direction due to its superior background correction capabilities. In this study, a method has been developed for the determination of Pb in road dust using HR-CS GF AAS and direct solid sample analysis. The analytical lines at 261.418 nm (2.1% relative sensitivity), with detection of 1 pixel, and at 283.306 nm (42% relative sensitivity), with side pixel evaluation, were used for Pb determination. Pyrolysis and atomization temperatures were 900 °C and 2300 °C, respectively, using a mixture of Pd and Mg as the chemical modifier. Twelve samples and three certified reference materials (CRMs) have been analyzed. A significant structured background has been observed at the optimum atomization temperature, which overlapped with the analyte atomic absorption wavelength. The background has been identified as AlCl, SiO and SiS molecules at 261.418 nm, and SiS at 283.306 nm. Least-squares background correction (LSBC) has been applied after the identification of the diatomic molecules and the results obtained for the CRMs were in agreement with the certified ones. The use of this correction technique allowed the elimination of spectral interference in the determination of Pb in road dust.

Received 11th December 2017
Accepted 16th February 2018

DOI: 10.1039/c7ja00405b

rsc.li/jaas

1. Introduction

The ever-increasing vehicle traffic circulation around the world has caused an increase in environmental pollution. Thus, the determination of traffic-related elements (TREs), especially potentially toxic metals, in environmental samples has grown in recent years, mainly due to the toxicity and persistence of these elements in the environment.[1,2] Many studies have detected the presence of TREs in airborne particulate matter, road dust, soil, plants, river sediments and other related matrices in several cities, using different analytical techniques and sample preparation procedures.[3–6]

Road dust can be considered a valuable indicator of environmental pollution. Harmful substances emitted by wear and exhaust from vehicles are deposited and accumulated in road dust, together with primary and secondary particles from other anthropogenic (demolition, construction, and industrial stacks) and natural sources (transport of resuspended soil). It can be considered a hazardous carrier of toxic metals, metalloids, and organic compounds that can be easily resuspended back into the atmosphere. Exposure to these emissions has been associated with adverse health effects and an increased risk of respiratory illnesses, demonstrating the importance of studying the chemical composition of this matrix.[3,7]

The enrichment of lead in roadside environments was a special concern in the 1970s due to the use of leaded fuels. After phasing out leaded gasoline, Pb was still present in airborne particulate matter and road dust due to its loss from

[a]Instituto de Química, Universidade Federal do Rio Grande do Sul, Porto Alegre, RS, Brazil. E-mail: mgrvale@ufrgs.br
[b]Comisión Nacional de Energía Atómica (CNEA), Gerencia Química, Consejo Nacional de Investigaciones Científicas y Técnicas – (CONICET), Buenos Aires, Argentina
[c]Instituto Nacional de Ciência e Tecnologia do CNPq–INCT de Energia e Ambiente, Universidade Federal da Bahia, Salvador, BA, Brazil
[d]Departamento de Química, Universidade Federal de Santa Catarina, Florianópolis, SC, Brazil

† Electronic supplementary information (ESI) available. See DOI: 10.1039/c7ja00405b

brake wear and wheel weights, which were considered as the main sources of vehicular Pb emission in the urban environment, although fuels still contain Pb at trace levels.[1,2]

The determination of the total analyte concentration in road dust, a complex matrix, usually involves an acid digestion procedure in the presence of nitric and hydrofluoric acids and, eventually, perchloric acid.[3,8,9] These digestion procedures enable sample decomposition, reducing matrix effects during the analysis, but they are relatively time-consuming and have risks of contamination and/or analyte loss, and the highly acidic and oxidative matrix attacks graphite tubes and reduces their lifetime. In this context, direct analysis of solid samples (SSs) offers important advantages in comparison with wet chemical approaches, such as increased detection power, as samples are not diluted, the absence of a corrosive matrix and waste, and the requirement of smaller amounts of sample, normally only a few milligrams.[10,11]

Among the techniques that can be used for SSs, graphite furnace atomic absorption spectrometry (GF AAS) offers important features: it allows the analysis of a variety of matrices, and calibration with aqueous standard solutions, after careful program optimization, which is unusual for SS techniques.[11] In spite of these advantages, the technique shows some limitations, typically associated with spectral interference caused by the matrix of the sample that cannot be corrected properly by conventional line source (LS) AAS instruments.[12]

The introduction of high-resolution continuum source atomic absorption spectrometry (HR-CS AAS) has provided visibility of the spectral environment around the analytical line, in contrast to LS AAS, and it has brought new possibilities in this field, such as improved potential to detect and correct spectral overlaps produced by radiation absorption from other species. Background absorption is frequently caused by diatomic molecules, which have high dissociation energy and exhibit a pronounced fine structure. In these cases, it is necessary to identify the interfering molecule in order to create the appropriate reference spectrum for correction using a least-squares background correction (LSBC) algorithm.[11,13]

Applications reporting the use of LSBC have been described in the literature since the first paper published by Becker-Ross *et al.*,[14] in which two spectral interferents (NO and PO) were identified and successfully corrected, allowing the determination of As and Se in human urine. Many of these studies were devoted to method development for direct analysis.[15–19] Araujo *et al.*[15] observed significant background absorption with pronounced rotational fine structure in the determination of antimony in sediments using direct solid sample analysis, caused by SiO and PO molecules. When more than one species is involved in the interference, LSBC is applied sequentially for each molecule. Borges *et al.*[16] investigated spectral interference in the determination of lead in fertilizers and limestone samples. The best results were found using a reference spectrum of the combination of different species (H_2SO_4 + Ca and HNO_3 + Ca solutions) at 283.306 nm. Although the interference was completely corrected using LSBC, the interfering molecules were not identified; the interference was attributed to molecules containing S and N in their structures.

The goal of this study has been to develop a fast routine analytical method for the determination of lead in road dust samples using HR-CS SS-GF AAS. The visibility of the spectral environment at high resolution in HR-CS AAS has also been used as a diagnostic tool in order to investigate and identify spectral interferents.

2. Materials and methods

2.1 Instrumentation

All measurements have been carried out using a high-resolution continuum source atomic absorption spectrometer model contrAA 700 (Analytik Jena AG, Jena, Germany). This instrument is equipped with a flame and a transversely heated graphite tube atomizer in two different sample compartments, and a high-intensity xenon short-arc lamp (300 W) operating in a hot-spot mode. The high resolution is achieved by combining a high-resolution double monochromator (prism and echelle grating) with a linear charge-coupled device (CCD) array detector with 588 pixels.

All experiments were carried out using pyrolytically coated SS graphite tubes without a dosing orifice (Analytik Jena, part no. 407-A81.303) and SS graphite platforms (Analytik Jena, part no. 407-152.023). An M2P microbalance (Sartorius, Göttingen, Germany) was used for weighing the samples directly onto the SS platform. A model SSA 6 manual solid sampling accessory (Analytik Jena) with a pre-adjusted pair of tweezers was used to transfer the SS platforms into the atomizer.

The analytical lines at 261.418 nm (2.1% relative sensitivity), with detection of 1 pixel, and at 283.306 nm (42% relative sensitivity), with side pixel evaluation at the line wings, were used for lead determination. Argon with a purity of 99.996% (White Martins, São Paulo, Brazil) was used as the purge and protective gas with a flow rate of 2.0 L min^{-1} during all stages, except during atomization when the flow was stopped. The graphite furnace temperature program used for all determinations is shown in Table 1.

2.2 Reagents

Analytical grade reagents were used exclusively. Deionized water with a specific resistivity of 18 MΩ cm from a Milli-Q water purification system (Millipore, Bedford, MA, USA) was used to prepare analytical solutions and dilutions. The aqueous standard solutions were prepared by dilutions of a 1000 mg L^{-1} Pb stock solution (SpecSol, São Paulo, Brazil) in 0.014 mol L^{-1}

Table 1 Temperature program for the determination of Pb in road dust samples by HR-CS SS-GF AAS

Stage	Temperature/°C	Ramp/°C s^{-1}	Hold time/s	Gas flow rate/L min^{-1}
Drying	90	10	20	2
Drying	130	10	40	2
Pyrolysis	900	300	30	2
Atomization	2300	3000	5	0
Cleaning	2450	500	5	2

HNO_3 (Anidrol, São Paulo, Brazil), previously purified by subboiling distillation in a quartz still (Marconi, Piracicaba, Brazil). The chemical modifier was a solution of 0.1% Pd + 0.06% Mg + 0.05% Triton X-100 (Pd and Mg as nitrates from Merck, Darmstadt, Germany and Triton X-100 from Union Carbide, Houston, TX, USA; all concentrations are % m/v).

2.3 Samples and certified reference materials

Twelve road dust samples were collected in the megacity of Buenos Aires, Argentina, in zones with different urban characteristics and traffic patterns. The dust sampling was from pavement edges using a broom and shovel (one set for each sample to avoid contamination). Each sample was put in a plastic bag. Once in the laboratory, the samples were dried at 100 °C for 24 h and fractionated by particle size, between 37 and 50 μm. More details about the sampling are provided in the study of Fujiwara *et al.*[3]

The following certified reference materials (CRM) were used for the evaluation of the accuracy of the method: NIST 2586, Trace Elements in Soil Containing Lead from Paint (National Institute of Standards and Technology, Gaithersburg, MD, USA); SO-2, Soil (Canada Centre for Mineral and Energy Technology, Ottawa, Canada); and BCR-723, Road Dust (European Commission Joint Research Centre, Institute for Reference Materials and Measurements, Geel, Belgium).

3. Results and discussion

3.1 Wavelength selection and pixel numbers evaluated

Due to the high lead content in the samples, two different approaches were studied to adjust the sensitivity to the linear range: an alternative line at 261.418 nm and the use of side pixels at 283.306 nm were evaluated. These secondary lines of Pb have 2.1% and 42% of relative sensitivity, respectively, in comparison with the most sensitive line at 217.001 nm.

The method developed here has been based on the integrated absorbance (A_{int}) values and the use of the IBC-m (iterative baseline correction for the monitoring of molecules) mode for setting the baseline. The exact details of this correction algorithm have not been disclosed yet, but its application helps in reducing the width of the lines at the cost of reducing the peak area.[11,20,21]

The A_{int} values were obtained using only the center pixel (CP) for the analytical line at 261.418 nm (slope = 0.00327 s ng^{-1}), and side pixel registration at the line wings to decrease the sensitivity and increase the working range at 283.306 nm. The pixels +4, −4 (slope = 0.00999 s ng^{-1}) and +5, −5 (slope = 0.00593 s ng^{-1}) were chosen for quantification.

The method was optimized using the analytical line at 261.418 nm. The optimum conditions were then used for the measurements at 283.306 nm.

3.2 Evaluation of the chemical modifier, temperature program, and sample mass

Due to the low thermal stability of Pb, the use of a chemical modifier is frequently reported in the literature, allowing the use of higher pyrolysis temperatures. The use of palladium and magnesium nitrates (Pd/Mg) as a chemical modifier for GF AAS was reported for the determination of Pb in different matrices.[22,23] In this study, the use of the Pd/Mg solution as a chemical modifier was investigated for Pb determination in road dust samples.

The optimum mass of the Pd/Mg modifier was investigated using a solution of 0.1% m/v Pd + 0.06% m/v Mg + 0.05% v/v Triton X-100, increasing the volume of the solution added from 0 to 25 μL, and Pd and Mg mass between 5 and 25 μg, and 3 and 15 μg, respectively. The use of Pd/Mg as a modifier caused an increase of about 30% in integrated absorbance, compared with no modifier. However, no significant variation has been observed between the different masses of the modifier. A mixture of 10 μg Pd + 6 μg Mg has been chosen to stabilize the analyte and it was employed in all further experiments.

The graphite furnace temperature program has been optimized using the M112-C road dust sample and an aqueous standard solution with 100 ng Pb. Fig. 1 shows the Pb pyrolysis and atomization curves. A plateau is observed up to a pyrolysis temperature of 900 °C for the sample and 1300 °C for the standard solution. Therefore, a temperature of 900 °C has been used in all further experiments to make sure that no analyte is lost in this program stage. In the optimization of the atomization temperature, the highest integrated absorbance values and best peak shapes have been obtained at 2300 and 2400 °C for both road dust sample and standard solution. An atomization temperature of 2300 °C has been chosen for the determination of Pb in order to increase the tube and platform lifetime.

After the temperature program optimization, the influence of the sample mass, weighed onto the SS platform and introduced into the graphite tube, has been investigated. A linear correlation (R = 0.9848) between the sample mass and integrated absorbance has been obtained evaluating masses from

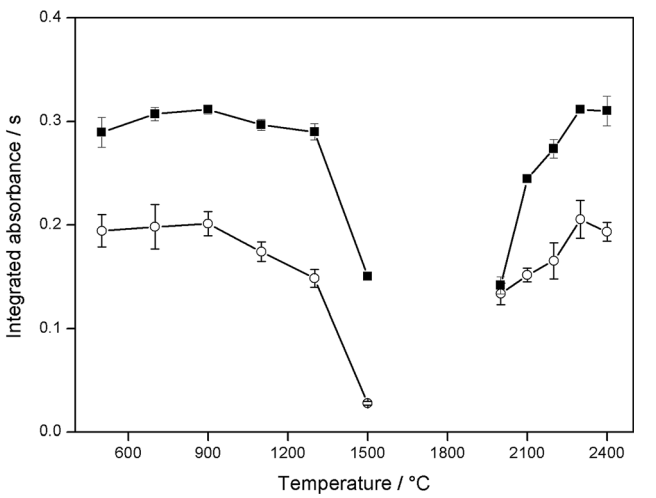

Fig. 1 Pyrolysis and atomization curves of Pb using 10 μg Pd + 6 μg Mg as the chemical modifier. (■) 100 ng Pb aqueous standard solution and (○) M112-C road dust sample (A_{int} values normalized to a mass of 0.3 mg). T_{atom} for pyrolysis curves = 2300 °C; T_{pyr} for atomization curves = 900 °C. Error bars correspond to the standard deviation (n = 5).

0.05 to 1 mg of the M112-C road dust sample. Hence, the maximum sample mass used in this work was limited to 1 mg.

3.3 Background identification and correction

The correction for continuous events, such as radiation scattering or molecular absorption due to dissociation continua of polyatomic molecules, is carried out automatically by the software of the HR-CS AAS instrument, using correction pixels. After this correction, only a structured background produced by absorption of radiation from other species, such as atoms and diatomic molecules, is displayed by the equipment.[11,15] In many cases, the interference can be eliminated using chemical modifiers and an optimized temperature program, or correction using reference spectra and LSBC.[14]

In this work, it was not possible to separate the analyte and interferent's signals. When the atomization temperature was lower than 2100 °C, the interference decreased, but the signal did not return to the baseline, which might indicate an overlap of the signals.

It has to be mentioned that the fine-structured background depended on the chemical composition of each sample. In this study, a structured background was observed for all samples and CRMs. The time-resolved absorption spectrum obtained for CRM SO-2 in the vicinity of the lead wavelength of 261.418 nm is shown in Fig. 2. The Pb atomic absorption line is marked with an arrow and all the other structures (peaks) are part of the electronic transition of one or more diatomic molecules with a pronounced rotational fine structure. The molecular bands overlapped with the atomic absorption of Pb to different degrees, depending on the molecule, interfering with the integrated absorbance value recorded for Pb. Different profiles were observed due to the presence of more than one diatomic molecule.

The identification of the molecular structures presented in this study is based on: (i) molecular data listed by Pearse & Gaydon,[24] such as the presence of electronic transitions in the vicinity of the Pb analytical line; (ii) information about the composition of the matrix;[3] (iii) the software database of the spectrometer (ASpect CS); and (iv) literature data about HR-CS molecular absorption spectrometry.[25–29] All spectra were obtained using the temperature program described in Table 1.

3.3.1 AlCl molecule. The AlCl molecule has been identified using the software database of the spectrometer (ASpect CS) and confirmed by evaluating the spectrum of an aqueous Al standard solution with HCl, shown in Fig. 3A. This molecule has an absorption band in the vicinity of 261.44 nm, which corresponds to the vibronic transition $X^1\Sigma^+ \rightarrow A^1\Pi(0 \rightarrow 0)$.[24] It displays narrow and very close bands, which are in part due to an isotopic splitting of the AlCl line,[25] which cannot be resolved by the HR-CS AAS equipment, so a single broad band is observed in the spectrum.

Fechetia *et al.*[26] determined chlorine in food samples using the molecular absorption of AlCl at the 261.418 nm wavelength, which overlaps with the analytical line of Pb, evaluated in this study. Another piece of evidence for AlCl molecule formation is the high concentration of Al in the CRMs evaluated (between 3.75 and 8.07% m/m).

The reference spectra and the LSBC were applied for AlCl after its identification. It can be seen in Fig. 3 that the AlCl

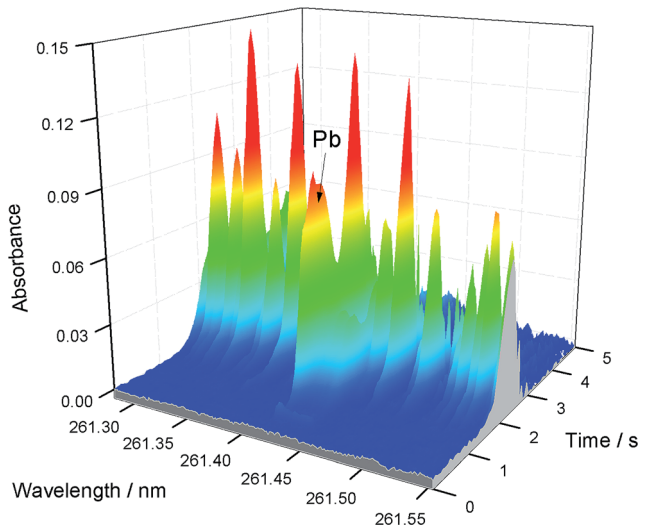

Fig. 2 Time-resolved absorption spectrum in the vicinity of the Pb line at 261.418 nm for 0.6 mg of CRM SO-2, using 10 μg Pd + 6 μg Mg as the chemical modifier. T_{pyr} = 900 °C and T_{atom} = 2300 °C.

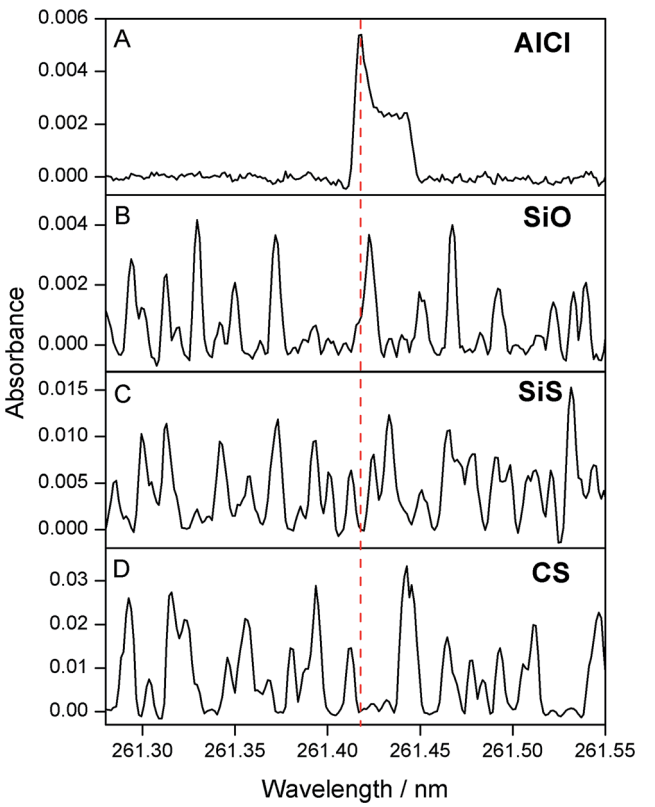

Fig. 3 Absorption spectra of AlCl, SiO, SiS, and CS in the vicinity of the Pb line at 261.418 nm for (A) 0.4 μg of Al and 8 μg of HCl; (B) 0.2 mg of silica; (C) 0.1 mg of Na_2SO_4 and 2 μg of Si; (D) 0.5 mg of Na_2SO_4, using 10 μg Pd + 6 μg Mg as the chemical modifier. T_{pyr} = 900 °C and T_{vap} = 2300 °C. The dashed line indicates the position of the analytical line of Pb (CP).

molecule is the main interferent at the analytical line for Pb, leading to an increase between 10 and 50% of the integrated absorbance, depending on the concentration of Pb and AlCl.

3.3.2 SiO molecule. Fujiwara *et al.*[3] evaluated the composition of the same street dust samples that were analyzed in the present work, by X-ray diffraction: quartz, clay aggregates, albite, anorthite, calcite, gypsum, iron and titanium oxide were detected. Individual street dust particles were characterized by scanning electron microscopy and energy dispersive X-ray analysis, showing that sulfur tended to reside on the particle surface, while Al, Ca, Mg, K, Fe and Si belonged to the lattice. Road dust is a silicate-rich matrix (quartz), and thus the SiO molecule was investigated. SiO has an absorption band at 261.13 nm, which corresponds to the vibronic transition $X^1\Sigma^+ \rightarrow A^1\Pi(5 \rightarrow 2)$.[24] Fig. 3B shows the absorption spectrum of the diatomic molecule SiO, which was confirmed to be an interfering molecule by analysis of the spectrum of pure silica. The high concentration of Si in the evaluated CRMs (between 24.99 and 29.15% m/m) is another piece of evidence for the formation of this molecule.

Practically all samples and CRMs exhibited interference of AlCl and SiO, except for BCR-723 (only AlCl). The use of LSBC allowed the elimination of the spectral interference through the sequential subtraction of each of the two molecules, making possible the determination of Pb. Fig. 3 shows that the SiO molecule has a smaller influence on the analytical line of Pb compared to AlCl, resulting in an increase between 1 and 10% of the integrated absorbance, depending on the concentration of Pb and SiO.

3.3.3 SiS molecule. The presence of another diatomic molecule has been observed during the analysis of CRM BCR-723, with a different profile compared to those of AlCl and SiO (Fig. 3C). This spectrum has been attributed to SiS.

Recently, Huang *et al.*[27] reported a study on sulfur determination *via* molecular absorption of SiS using an experimental setup including a commercial contrAA 700 spectrometer and a modular simultaneous echelle spectrograph (MOSES). The absorption spectrum of SiS was investigated over a broad wavelength range between 200 and 735 nm. The authors observed a strong structured molecular absorption between 200 and 320 nm, which was attributed to the absorption from two diatomic molecules, namely SiO between 200 and 260 nm, and SiS between 260 and 320 nm.

Fig. S1† compares the absorption spectrum of SiS in the vicinity of the Pb line at 261.418 nm obtained by the current method using HR-CS AAS (Fig. S1A†), and the one obtained using the MOSES spectrograph (Fig. S1B,† data provided by ISAS Berlin), confirming the identity of the interfering molecule.

SiS did not interfere significantly with the analytical line of Pb (Fig. 3): its contribution to the A_{int} of Pb in BCR-723 was approximately 0.05%, which could be barely classified as interference. Nonetheless, the knowledge of an interfering species is important because the magnitude of the interference depends on the concentration of both analyte and interferent.

3.3.4 CS molecule. During the generation of the reference spectrum of SiS, the formation of another diatomic molecule has been observed, shown in Fig. 3D, which has been identified as the CS molecule. The identification was not straightforward because three molecules, CS, SO, and S_2, could be generated and absorb in this region. Clearly, other species could absorb in this region as well; however, preliminary tests have shown that this molecule contains sulfur.

Katskov *et al.*[28] investigated the formation of these molecules in the 187–380 nm range by the vaporization of sulfur, sulfuric acid and sulfur compounds (sulfates and sulfides) using a medium-resolution UV-spectrometer with a CCD array detector, a deuterium lamp as the radiation source, and a graphite tube vaporizer. The authors observed two spectra, structured and diffuse, attributed to S_2 and SO, respectively. The S_2 spectrum was characterized by a single dominating system consisting of diffuse bands overlapping with sharp lines with a band head at approximately 275 nm. The SO absorption spectrum consisted of two diffuse bands, with maxima approximately at 218 and 290 nm. The spectrum at 250–270 nm was correlated with the CS molecule. In another study,[29] the authors investigated alkali metal sulfates and sulfides using the same technique. The authors observed three discrete band systems with a dominating maximum at 258.8 nm attributed to the CS molecule.

In order to identify the diatomic molecule, a Na_2SO_4 solution was evaluated at different wavelengths: 275 nm for S_2, 218 and 290 nm for SO, and 258.8 nm for CS. It is important to emphasize that this molecule has been observed even when Si was not added for the measurements. The same peak profile, considering the time-resolved spectrum, was observed at 258.800 and 261.417 nm; thus the molecule generated has been identified as CS.

The influence of the Si mass on the SiS and CS generation has been investigated using sodium sulfate and sulfuric acid solutions. The masses evaluated were 60 μg S and between 0.25 and 3 μg Si. The profiles of both molecules by wavelength are distinct and Fig. 4 shows the transient signals of these molecules recorded at 261.439 nm from 1.1 to 3.9 s. Particulates have scattered the radiation before 1 s in the atomization stage, which has led to an anomalous profile without molecule information.

Fig. 4A shows the absorption profiles obtained for the sodium sulfate solution. The CS molecule was observed with and without Si, and the integrated absorbance remained constant. The SiS formation was observed from the addition of 0.25 μg of Si and the absorption signal increased with increasing addition of Si.

Sulfuric acid solution was evaluated and its absorption profiles are shown in Fig. 4B. In the absence of Si, none of the molecules was generated. SiS could only be observed with Si mass higher than 0.25 μg, and CS with the addition of 1 μg Si. In both cases, the absorption peaks increased with increasing addition of Si. The formation of the CS molecule only with the addition of Si demonstrates the performance of Si as a chemical modifier. The separation in time between SiS and CS shown in Fig. 4 was only possible using a graphite platform after about 100 heating cycles. When a new graphite platform was used, the absorption peaks of SiS and CS overlapped.

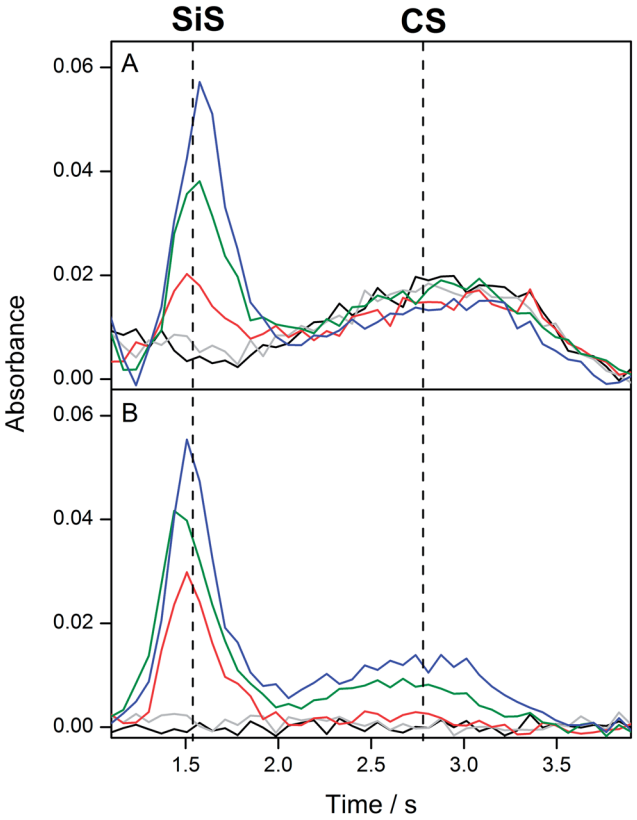

Fig. 4 Influence of the mass of Si on the SiS and CS generation, using 60 mg of (A) sodium sulfate and (B) sulfuric acid; black line: without Si; grey line: with 0.25 mg Si; red line: with 1 mg Si; green line: with 2 mg Si; and blue line: with 3 mg Si. T_{pyr} = 900 °C and T_{vap} = 2300 °C. Transient signals were recorded at 261.439 nm (pixel 116).

The results demonstrated the distinct behavior of different sulfur compounds in the generation of CS. For this reason, the CS formation was evaluated for additional organic and inorganic reagent solutions: $MnSO_4$, Na_2S, L-cysteine, thiourea, sulfamic acid and H_2SO_4.

The CS generation was observed only for Na_2SO_4, $MnSO_4$, and Na_2S. This is most likely due to the difference in the thermal stability of inorganic and organic compounds.

Mior *et al.*[30] investigated the determination of sulfur in coal *via* the molecular absorption of CS at 258.033 nm using direct solid sample analysis with calibration against aqueous standard solutions. They investigated inorganic ($MgSO_4$) and organic (L-cysteine) sulfur compounds as possible standards, using Ru as a permanent chemical modifier. They observed that the thermal behavior of the two standards was significantly different. The magnesium sulfate solution showed a high thermal stability, while the L-cysteine solution exhibited decreasing sensitivity over the entire pyrolysis temperature range, which was more similar to the behavior of the coal samples.

With the addition of a Pd/Mg (10/6 μg) mixture, the chemical modifier used in this study, the CS generation was observed for all organic and inorganic sulfur compounds. Studies have demonstrated a strong tendency of Pd to interact with sulfur, thus helping in breaking the original sulfur bonds and stabilizing the sulfur.[20,31] However, a different behavior has been observed for each sulfur species. Masses of 20 μg S, and 10 μg Pd + 6 μg Mg, the chemical modifier used in this study, were evaluated. Pixel 119 (λ = 261.443 nm) was monitored because it presented the highest signal.

Different sensitivities were obtained on varying the sulfur compound analyzed, Na_2S > Na_2SO_4 > L-cysteine > $MnSO_4$ > H_2SO_4 > thiourea > sulfamic acid. The difference in integrated absorbance between the most sensitive (Na_2S) and the least sensitive (sulfamic acid) was approximately 13 times, which demonstrates the importance of choosing a suitable sulfur species for calibration.

The melting point (MP) of all the tested compounds differs from each other. The inorganic species are less volatile, Na_2S (MP 1172 °C), Na_2SO_4 (MP 884 °C), and $MnSO_4$ (MP 700 °C), whereas the organic species have lower MP temperatures, thiourea (MP 178 °C), sulfamic acid (decomposes at 205 °C), and L-cysteine (decomposes at 240 °C).[32] The results demonstrated that the modifier stabilized better the inorganic species, and did not offer the same performance for the organic species. The behavior of L-cysteine is probably related to the availability of the S atom in the structure of this compound, enabling easier interaction with the chemical modifier and the generation of carbon monosulfide. The S atom has only sigma-bonds in this compound, while in the other organic species it has pi-bonds, with higher bond strength.

Another evaluated condition for SiS and CS generation was the medium (acidic or basic) of the Si standard. Sodium sulfate and sulfuric acid solutions were studied: 60 μg S and 1 to 20 μg Si. The Si solutions were prepared by dilution of a stock solution of 1000 mg L^{-1} Si in HNO_3 and HF, and another one in NaOH.

In the sodium sulfate solution, with the addition of the Si standard in acidic or basic medium, the generation of both molecules has been observed; however, the generation of SiS is favored using the Si standard in NaOH.

For sulfuric acid solution, the addition of the Si standard in NaOH has generated both molecules. The addition of 1 and 2 μg of Si standard in HNO_3 and HF could not support the formation of molecules, but on adding higher Si masses of 3 to 20 μg, the CS molecule was observed. It is noteworthy that no further C source was added; therefore Si could act as a chemical modifier for CS generation.

The SiS molecule was generated only with the addition of the Si standard in basic medium. This is probably due to the reaction between H_2SO_4 and NaOH, leading to the formation of Na_2SO_4, which is less volatile compared with H_2SO_4. The addition of 6.8 μg of KOH, together with the acid Si standard, has shown the same behavior observed when a basic Si solution was studied.

3.4 Side pixel registration

For comparison purposes, measurements at 283.306 nm were carried out, with side pixel evaluation at the line wings. Side pixel registration can be used to reduce the sensitivity and increase the working range without the need for making additional measurements or dilutions.[33–36] Heitmann *et al.*[33] demonstrated the possibility of expanding the linear range of the calibration curve using less sensitive side pixels, which was

also used in another study on Zn determination.[34] The use of an Ar flow in the atomization stage is another solution frequently used to decrease the sensitivity.[11] In this study, a gas flow rate of 0.1 L min^{-1} has been used in the atomization stage, but the concentrations found for the CRM were not in agreement with the certified values, indicating that this measure could not be used in the present case to reduce the sensitivity.

In the measurements carried out at 283.306 nm, a structured background was again observed for all samples and CRMs. In order to identify the diatomic molecule, L-cysteine was evaluated. The formation of two different molecules has been observed, depending on the heating cycle of the graphite furnace. Fig. 5 shows the absorption spectra obtained for L-cysteine and Pd/Mg as the chemical modifier in the vicinity of the lead line at 283.306 nm, over two time intervals, from 0 to 1.1 s (Fig. 5A) and from 1.1 to 5.0 s (Fig. 5B), using a graphite platform after some heating cycles. The different profiles were due to the presence of more than one diatomic molecule. However, when a new platform was used, only the spectrum depicted in Fig. 5A has been observed, and without the addition of Pd/Mg as the chemical modifier none of the molecules was generated.

In order to identify the diatomic molecules generated, a sodium sulfite solution was evaluated, without and with the addition of a Si standard solution, using a new graphite platform. Both spectra were obtained with the addition of the Si standard solution and only the spectrum in Fig. 5A was obtained without the addition of a Si standard solution. Thus, the spectrum shown in Fig. 5A has been attributed to CS and that in Fig. 5B to SiS. The CS molecule has an absorption band at 283.680 nm, which corresponds to the vibronic transition $X^1\Sigma^+ \rightarrow A^1\Pi(7 \rightarrow 5)$.[24]

The generation of SiS using only L-cysteine and Pd/Mg as the chemical modifier occurred probably due to the deposition of the Si onto the platform as a kind of permanent modifier.

The absorption profiles of both molecules are distinct and Fig. 6 shows the transient signals of these molecules recorded at 283.346 nm from 0 to 2.5 s, obtained for sodium sulfite and a Si standard solution. The separation in time of CS and SiS was only possible using a graphite platform after some 100 heating cycles. When a new platform was used, a spectral overlap in time has been observed.

Fig. S2† compares the absorption spectrum of SiS in the vicinity of the Pb line at 283.306 nm obtained by the current method using HR-CS GF AAS (Fig. S2A†) and the one obtained using the MOSES spectrograph (Fig. S2B,† data provided by ISAS Berlin), confirming the identity of the interfering molecule.

After identifying the spectral interference, the reference spectra of SiS and the LSBC were applied for the CRMs and samples, except for NIST 2586, because, in spite of the high Si content of this CRM, it did not show any interference due to SiS, probably because of its low sulfur content. Fig. 7 shows the correction for the CRM BCR-723. It can be seen that the location of the maximum absorbance of SiS coincides with the pixels chosen for the determination of Pb, resulting in an increase between 2 and 35% of the integrated absorbance, depending on the concentration of Pb and SiS and the pixel evaluated.

3.5 Figures of merit

Calibration curves were established with a blank and six Pb standards, ranging from 0.5 to 10 mg L^{-1} (5–100 ng) in 0.014 mol L^{-1} HNO_3. The limit of detection (LOD) and the limit of quantification (LOQ) were calculated as three and ten times the standard deviation of 10 measurements of a blank, respectively, divided by the slope of the calibration curve. The blank measurements were carried out according to the "zero mass response" principle,[37] using only the modifier (10 μL of the solution of 0.1% m/v Pd + 0.06% m/v Mg + 0.05% v/v Triton X-100) on the SS platform. The characteristic mass (m_0) is defined as the mass of the analyte corresponding to an integrated absorbance of 0.0044 s. The figures of merit of the developed method are summarized in Table 2. For the analytical

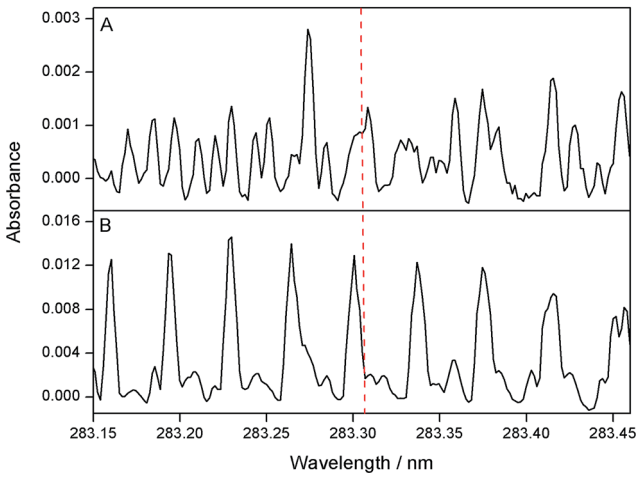

Fig. 5 Absorption spectrum in the vicinity of the Pb line at 283.306 nm for 0.4 mg of L-cysteine, using 10 μg Pd + 6 μg Mg as the chemical modifier. T_{pyr} = 900 °C and T_{atom} = 2300 °C. (A) Integration limits 0.0–1.1 s; (B) integration limits 1.1–5.0 s. The dashed line indicates the position of the analytical line (CP).

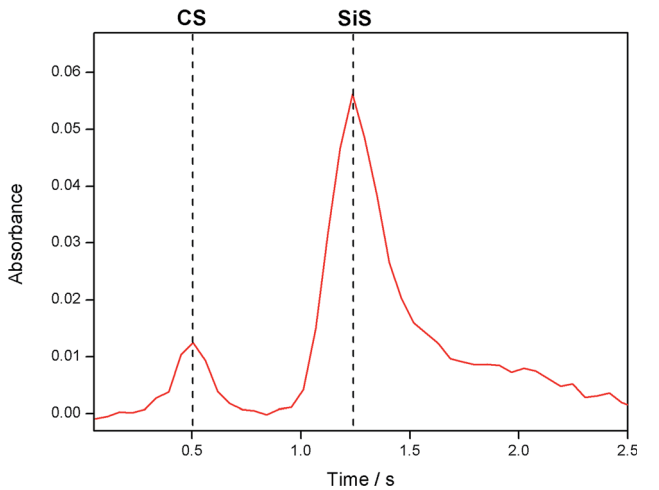

Fig. 6 Transient signals of CS and SiS recorded at 283.346 nm for a sodium sulfite solution (10 μg S) and 0.2 μg Si. T_{pyr} = 900 °C and T_{vap} = 2300 °C.

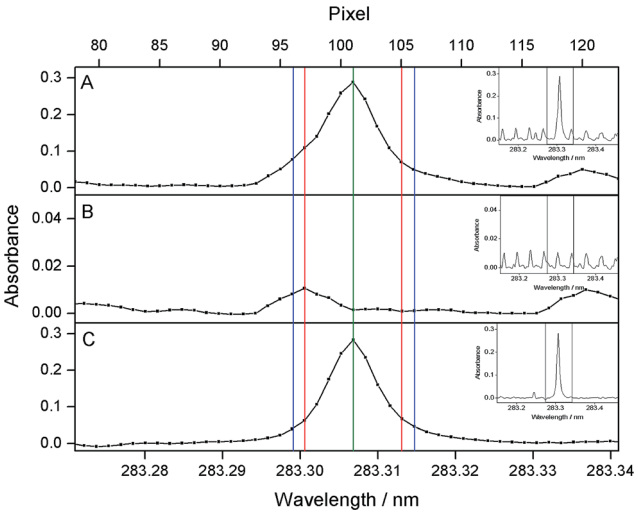

Fig. 7 Absorption spectrum (zoom) in the vicinity of the Pb line at 283.306 for (A) 0.099 mg of CRM BCR-723 (road dust); (B) 0.4 mg of L-cysteine; and (C) CRM BCR-723 with LSBC using the spectrum of CS as the reference and 10 mg Pd + 6 mg Mg as the chemical modifier. T_{pyr} = 900 °C and $T_{atom/vap}$ = 2300 °C. The spectrum for 200 pixels is shown in the right corner. The colored lines indicate the positions of the CP (green line), pixels +4,−4 (red lines) and pixels +5,−5 (blue lines).

line at 283.306 nm, the analytical performance is a function of the number and location of the pixels selected for quantification. The center pixel is marked with CP, and the side pixels with a number which indicates their distance to the CP. As can be seen, an increasing distance to the line core results in a significant reduction in sensitivity, and in an increase in linearity. The characteristic mass and the limit of detection also increase. The pixels +4, −4 and +5, −5 were chosen for quantification, because they presented the best linearity for the concentration range evaluated.

The characteristic mass value obtained is in agreement with the value found in the literature for Pb using the analytical line of 261.418 nm. Welz and Sperling[38] reported an m_0 of 1.0 ng using GF AAS with Zeeman-effect background correction and without any chemical modifier.

The LOD and LOQ presented in this study were calculated for the maximum sample mass weighed onto the SS platform, *i.e.*, 1 mg, and cannot be directly compared with those reported in the literature, since measures were taken to reduce the sensitivity of the measurement due to the high content of Pb present in the road dust samples, such as the use of the secondary analytical line at 261.418 nm and the use of side pixels at 283.306 nm.

3.6 Analysis of the CRMs and the road dust samples

Three CRMs were evaluated in order to check the accuracy of the developed method: NIST 2586 (soil); SO-2 (soil); and BCR-723 (road dust). The concentration values obtained for Pb were in agreement with the certified ones according to a Student's *t*-test

Table 2 Figures of merit for Pb determination in road dust samples by HR-CS SS-GF AAS, using 10 μg Pd + 6 μg Mg as the chemical modifier. T_{pyr} = 900 °C and T_{atom} = 2300 °C

Wavelength/nm	Pixel monitored	Slope/s ng^{-1}	R	m_0/ng	LOD[a]/mg kg^{-1}	LOQ[a]/mg kg^{-1}
261.418	CP	0.00327	0.9965	1.20	0.65	2.2
283.306	CP	0.02738	0.9335	0.10	0.03	0.11
	+1, −1	0.04570	0.9482	0.06	0.02	0.07
	+2, −2	0.02941	0.9713	0.10	0.03	0.11
	+3, −3	0.01731	0.9873	0.20	0.05	0.18
	+4, −4	0.00999	0.9960	0.38	0.09	0.31
	+5, −5	0.00593	0.9988	0.69	0.16	0.52

[a] LOD and LOQ calculated for 1 mg of sample.

Table 3 Results obtained for the determination of Pb in the CRMs, without and with LSBC, using HR-CS SS-GF AAS and 10 μg Pd + 6 μg Mg as the chemical modifier. T_{pyr} = 900 °C and T_{atom} = 2300 °C. P4 corresponds to pixels +4, −4 and P5 to pixels +5, −5 (mean ± sd, n = 5)

		Wavelength/nm				
		261.418		283.306		
		Found value/mg kg^{-1}			Found value/mg kg^{-1}	
CRM	Certified value/mg kg^{-1}	Without correction	With LSBC	Pixel monitored	Without correction	With LSBC
NIST 2586	432 ± 17	500 ± 37	435 ± 33	P4	431 ± 38	—
				P5	426 ± 33	
SO-2	21 ± 4	95 ± 12	24 ± 3	P4	24 ± 1	22 ± 1
				P5		23 ± 1
BCR-723	866 ± 16[a]	955 ± 54	860 ± 38	P4	1.228 ± 69	887 ± 61
				P5	1.267 ± 78	867 ± 48

[a] Informative value.

Table 4 Concentration of Pb in road dust samples, without and with LSBC, using HR-CS SS-GF AAS and 10 μg Pd + 6 μg Mg as the chemical modifier. T_{pyr} = 900 °C and T_{atom} = 2300 °C. P4 corresponds to pixels +4, −4 and P5 to pixels +5, −5 (mean ± sd, n = 5)

	Wavelength/nm				
	261.418		283.306		
	Pb concentration/mg kg^{-1}			Pb concentration/mg kg^{-1}	
Sample	Without correction	With LSBC	Pixel monitored	Without correction	With LSBC
M5-C	354 ± 40	179 ± 19	P4	175 ± 15	162 ± 16
			P5	180 ± 14	166 ± 15
M112-C	425 ± 48	231 ± 24	P4	256 ± 26	245 ± 24
			P5	259 ± 28	252 ± 25
M10-B	325 ± 32	172 ± 20	P4	167 ± 11	160 ± 9
			P5	170 ± 11	166 ± 8
M11-B	444 ± 47	273 ± 33	P4	262 ± 26	256 ± 25
			P5	262 ± 24	258 ± 24
M12-B	543 ± 66	341 ± 37	P4	333 ± 28	317 ± 29
			P5	330 ± 27	314 ± 30
M38-B	396 ± 33	260 ± 13	P4	289 ± 17	279 ± 17
			P5	292 ± 16	285 ± 17
M42-B	687 ± 74	442 ± 29	P4	478 ± 60	451 ± 57
			P5	491 ± 60	466 ± 58
M90-B	418 ± 33	182 ± 21	P4	196 ± 17	179 ± 18
			P5	194 ± 16	181 ± 17
M94-B	409 ± 45	176 ± 21	P4	184 ± 24	175 ± 24
			P5	181 ± 21	175 ± 20
M110-B	485 ± 46	293 ± 38	P4	346 ± 32	335 ± 33
			P5	354 ± 32	345 ± 34
M156-B	742 ± 76	528 ± 60	P4	582 ± 55	575 ± 56
			P5	571 ± 33	566 ± 34
M174-B	375 ± 32	225 ± 17	P4	218 ± 8	209 ± 8
			P5	220 ± 6	213 ± 5

at the 95% confidence level ($t_{calc} < t_{crit}$; t_{crit} = 2.8). The good agreement of the results confirms that the developed method is accurate and can be used to determine Pb in road dust samples. Table 3 shows both certified and experimental concentrations, without and with LSBC, and the values calculated using the Student's t-test (t_{calc}). Only for the CRM SO-2, using the pixels +5, −5 for quantification, $t_{calc} > t_{crit}$. Considering all the measurements, the relative standard deviation (RSD) values were typically around 10%, which is quite acceptable for this kind of samples.

Twelve samples of road dust were analyzed using direct solid sample introduction (Table 4). The concentrations varied between 160 and 575 mg kg^{-1}. Khairy *et al.*[8] showed the global concentrations of trace metals (mg kg^{-1}) in road dust in their study. The Pb concentrations varied between 1.4 (Karak, Jordan) and 4443 mg kg^{-1} (Shanghai, China).

The results obtained using both methods were compared using Analysis of Variance (ANOVA) and they were not significantly different at the 95% confidence level. These results confirm the accuracy of the methods and corroborate the possibility of using aqueous standards for calibration.

4. Conclusions

A procedure for the determination of lead in road dust samples has been developed using HR-CS GF AAS, direct solid sample analysis and calibration against aqueous standard solutions. The visibility of the spectral environment at high resolution has been used as a diagnostic tool in order to investigate and identify spectral interference. The spectral interference has been corrected using LSBC, making possible the accurate determination of Pb in a complex matrix such as road dust.

Conflicts of interest

There are no conflicts to declare.

Acknowledgements

The authors are grateful to the Conselho Nacional de Desenvolvimento Científico e Tecnológico (CNPq), the Instituto Nacional de Ciência e Tecnologia do CNPq – INCT de Energia e Ambiente, Salvador, BA, Brazil, and the Coordenação de Aperfeiçoamento de Pessoal de Nível Superior (CAPES) for scholarships and financial support. MGRV has a research scholarship from CNPq, grant no. 305679/2015-5; BW also has a research scholarship from CNPq, grant no. 303526/2016-5. The authors are also grateful to the research group of Helmut Becker-Ross, from ISAS Berlin, Germany, for providing the data obtained with the MOSES spectrograph.

References

1 P. Smichowski, D. Gómez, C. Frazzoli and S. Caroli, *Appl. Spectrosc. Rev.*, 2008, **43**, 23–49.
2 H. Zhang, Z. Wang, Y. Zhang, M. Ding and L. Li, *Sci. Total Environ.*, 2015, **521–522**, 160–172.
3 F. Fujiwara, R. J. Rebagliati, L. Dawidowski, D. Gómez, G. Polla, V. Pereyra and P. Smichowski, *Atmos. Environ.*, 2011, **45**, 1497–1505.
4 A. A. Shaltout, J. Boman, B. Welz, I. N. B. Castilho, E. A. Al Ashkar and S. M. Gaita, *Microchem. J.*, 2014, **113**, 4–9.
5 M. Werkenthin, B. Kluge and G. Wessolek, *Environ. Pollut.*, 2014, **189**, 98–110.
6 C. L. S. Wiseman, F. Zereini and W. Püttmann, *Environ. Sci. Pollut. Res.*, 2014, **21**, 1572–1581.
7 F. Amato, M. Pandolfi, M. Viana, X. Querol, A. Alastuey and T. Moreno, *Atmos. Environ.*, 2009, **43**, 1650–1659.
8 M. A. Khairy, A. O. Barakat, A. R. Mostafa and T. L. Wade, *Microchem. J.*, 2011, **97**, 234–242.
9 Y. Yu, Y. Li, B. Li, Z. Shen and M. K. Stenstrom, *Environ. Pollut.*, 2016, **216**, 764–772.
10 M. G. R. Vale, N. Oleszczuk and W. N. L. dos Santos, *Appl. Spectrosc. Rev.*, 2006, **41**, 377–400.
11 M. Resano, M. Aramendía and M. A. Belarra, *J. Anal. At. Spectrom.*, 2014, **29**, 2229–2250.
12 B. Welz, M. G. R. Vale, D. L. G. Borges and U. Heitmann, *Anal. Bioanal. Chem.*, 2007, **389**, 2085–2095.
13 B. Welz, S. Morés, E. Carasek, M. G. R. Vale, M. Okruss and H. Becker-Ross, *Appl. Spectrosc. Rev.*, 2010, **45**, 327–354.
14 H. Becker-Ross, S. Florek and U. Heitmann, *J. Anal. At. Spectrom.*, 2000, **15**, 137–141.
15 R. G. O. Araujo, B. Welz, F. Vignola and H. Becker-Ross, *Talanta*, 2009, **80**, 846–852.
16 A. R. Borges, E. M. Becker, L. L. François, A. de Jesus, M. G. R. Vale, B. Welz, M. B. Dessuy and J. B. de Andrade, *Spectrochim. Acta, Part B*, 2014, **101**, 213–219.
17 F. G. Lepri, D. L. G. Borges, R. G. O. Araujo, B. Welz, F. Wendler, M. Krieg and H. Becker-Ross, *Talanta*, 2010, **81**, 980–987.
18 D. L. G. Borges, A. F. da Silva, B. Welz, A. J. Curtius and U. Heitmann, *J. Anal. At. Spectrom.*, 2006, **21**, 763–769.
19 M. Resano, E. Mozas, C. Crespo, J. Briceño, J. d. C. Menoyo and M. A. Belarra, *J. Anal. At. Spectrom.*, 2010, **25**, 1864–1873.
20 Z. Kowalewska, *Spectrochim. Acta, Part B*, 2011, **66**, 546–556.
21 F. V. Nakadi, M. A. M. S. da Veiga, M. Aramendía, E. García-Ruiza and M. Resano, *J. Anal. At. Spectrom.*, 2016, **31**, 1381–1390.
22 G. Schlemmer and B. Welz, *Spectrochim. Acta, Part A*, 1986, **41**, 1157–1165.
23 A. R. Borges, E. M. Becker, M. B. Dessuy, M. G. R. Vale and B. Welz, *Spectrochim. Acta, Part B*, 2014, **92**, 1–8.
24 R. W. B. Pearse and A. G. Gaydon, *The identification of molecular spectra*, Chapman and Hall, London, 1976.
25 F. V. Nakadi, M. A. M. S. Da Veiga, M. Aramendia, E. Garcia-Ruiz and M. Resano, *J. Anal. At. Spectrom.*, 2015, **30**, 1531–1540.
26 M. Fechetia, A. L. Tognon and M. A. M. S. da Veiga, *Spectrochim. Acta, Part B*, 2012, **71–72**, 98–101.
27 M. D. Huang, H. Becker-Ross, S. Florek, C. Abad and M. Okruss, *Spectrochim. Acta, Part B*, 2017, **135**, 15–21.
28 D. A. Katskov, M. Lemme and P. Tittarelli, *Spectrochim. Acta, Part B*, 2004, **59**, 101–114.
29 M. Lemme, D. A. Katskov and P. Tittarelli, *Spectrochim. Acta, Part B*, 2004, **59**, 115–124.
30 R. Mior, S. Morés, B. Welz, E. Carasek and J. B. de Andrade, *Talanta*, 2013, **106**, 368–374.
31 M. Resano and M. R. Flórez, *J. Anal. At. Spectrom.*, 2012, **27**, 401–412.
32 D. R. Lide, *CRC Handbook of Chemistry and Physics*, Taylor and Francis, Boca Raton, 89th edn, 2009.
33 U. Heitmann, B. Welz, D. L. G. Borges and F. G. Lepri, *Spectrochim. Acta, Part B*, 2007, **62**, 1222–1230.
34 J. Briceño, M. A. Belarra, K. A. C. De Schamphelaere, S. Vanblaere, C. R. Janssen, F. Vanhaecke and M. Resano, *J. Anal. At. Spectrom.*, 2010, **25**, 503–510.
35 I. M. Dittert, J. S. A. Silva, R. G. O. Araujo, A. J. Curtius, B. Welz and H. Becker-Ross, *J. Anal. At. Spectrom.*, 2010, **25**, 590–595.
36 M. Resano, A. C. Lapeña and M. A. Belarra, *Anal. Methods*, 2013, **5**, 1130–1139.
37 U. Kurfürst, *Solid Sample Analysis – Direct and Slurry Sampling using GFAAS and ETV-ICP*, Springer-Verlag, Berlin, 1998.
38 B. Welz and M. Sperling, *Atomic Absorption Spectrometry*, Wiley-VCH, Weinheim, 1999.

